# THE ADS ALL-SKY SURVEY

*Alberto Pepe*
Postdoc, Harvard CfA
Co-founder, *Au*thorea

ACCOMAZZI
BORKIN
BURKE
CROSAS
D'ABRUSCO
DAVE'
ERDMANN
GOODMAN
KURTZ
LU
LUKER
MUENCH
PEPE

# SEAMLESS ASTRONOMY

at the CfA

DATA CITATION
# PRACTICES

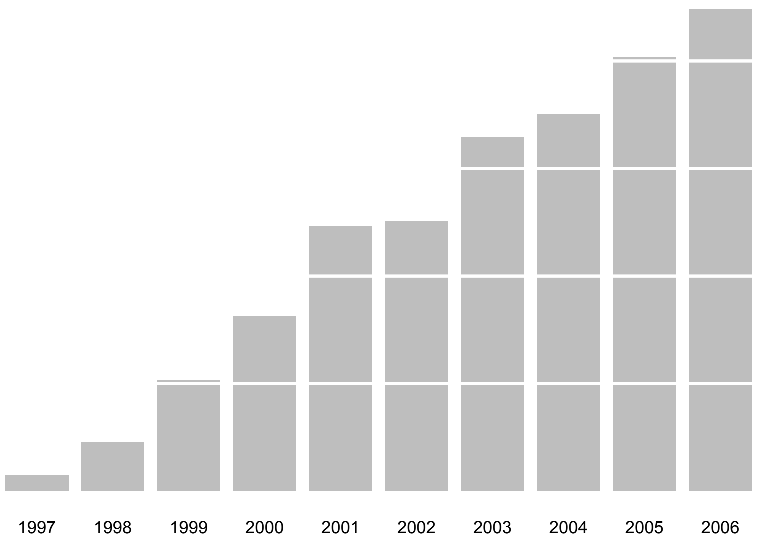


# of astronomy papers with links

# PLATFORMS

FOR DATA CITATION,
PUBLICATION, AND DISCOVERY

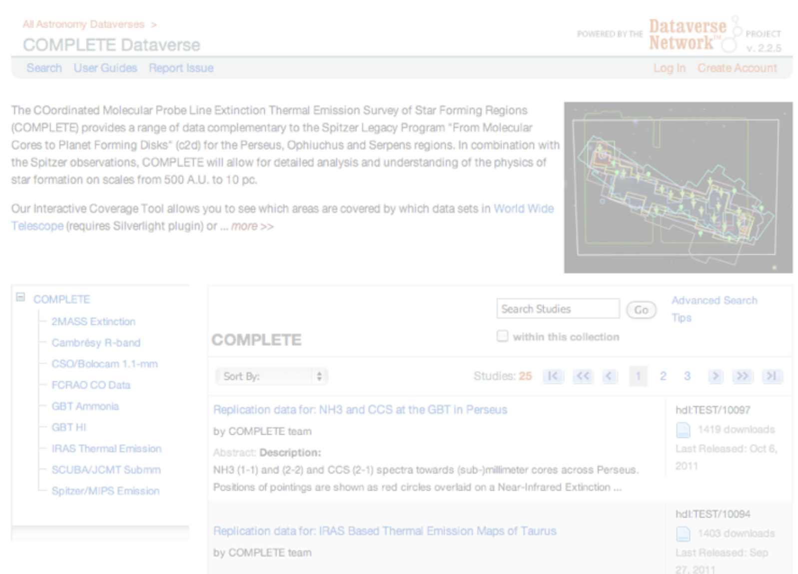


http://dvn.theastrodata.org

VISUALIZATION OF
COLLABORATION
# NETWORKS

http://adslabs.org

## DATA CITATION PRACTICES

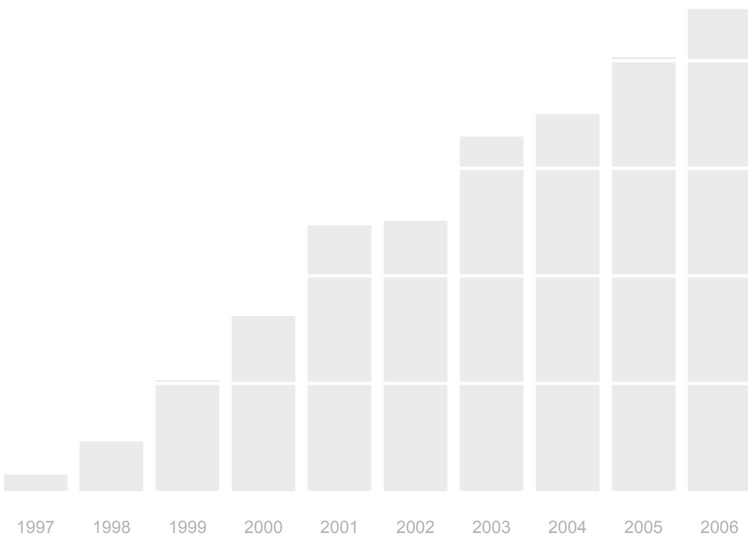


# of astronomy papers with links

## PLATFORMS FOR DATA CITATION, PUBLICATION, AND DISCOVERY

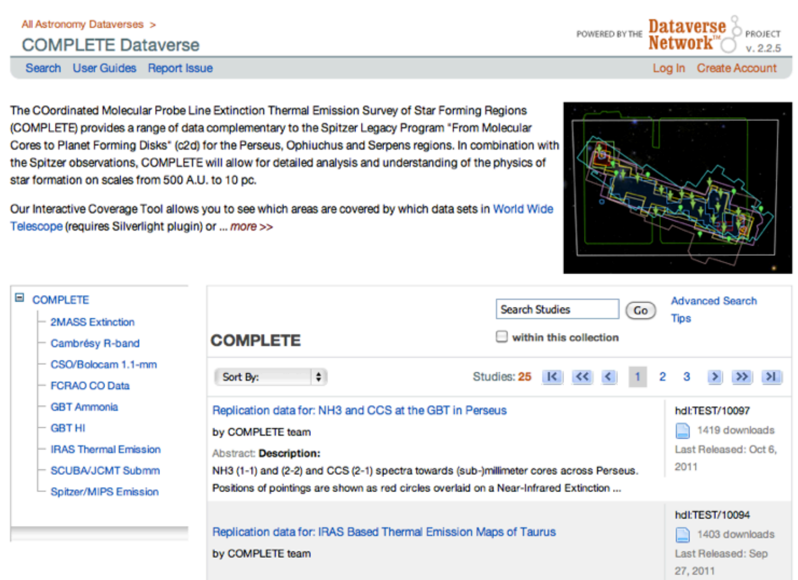


http://dvn.theastrodata.org

## VISUALIZATION OF COLLABORATION NETWORKS

http://adslabs.org

# DATA CITATION PRACTICES

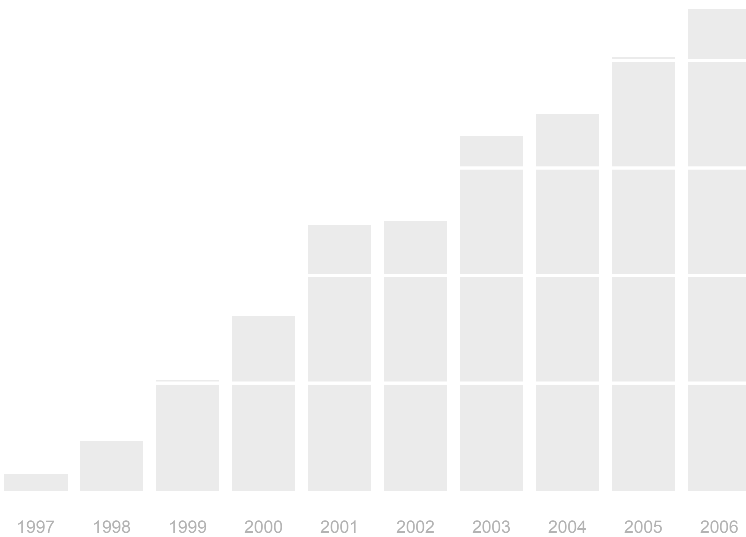


# of astronomy papers with links

# PLATFORMS

## FOR DATA CITATION, PUBLICATION, AND DISCOVERY


http://dvn.theastrodata.org

# VISUALIZATION OF COLLABORATION NETWORKS

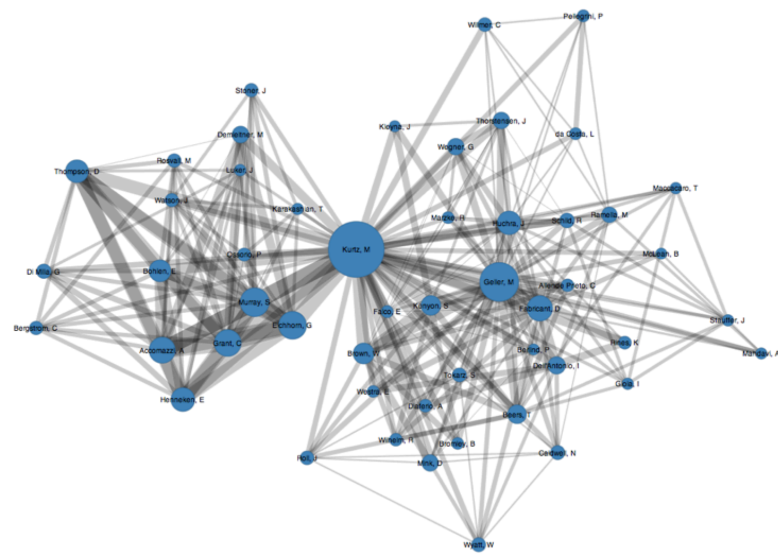

http://adslabs.org

ACCOMAZZI
BORKIN
BURKE
CROSAS
D'ABRUSCO
DAVE'
ERDMANN
GOODMAN
KURTZ
LU
LUKER
MUENCH
PEPE

# SEAMLESS ASTRONOMY
at the CfA

# ADS ALL-SKY SURVEY
Collaboration

**ACCOMAZZI**
BORKIN
BURKE
CROSAS
D'ABRUSCO
DAVE'
ERDMANN
**GOODMAN**
KURTZ
**LU**
LUKER
**MUENCH**
**PEPE**

**BOCH, GENOVA** (CDS)
**CONTI** (STScI)
**FAY** (MSR)
**HOGG, LANG** (Astrometry.net)

# THE ADS* ALL-SKY SURVEY

# THE ADS* ALL-SKY SURVEY

*Astrophysics **Data** System

see Murray et al.. (1992) in ESO Conference and Workshop Proceedings, vol. 43

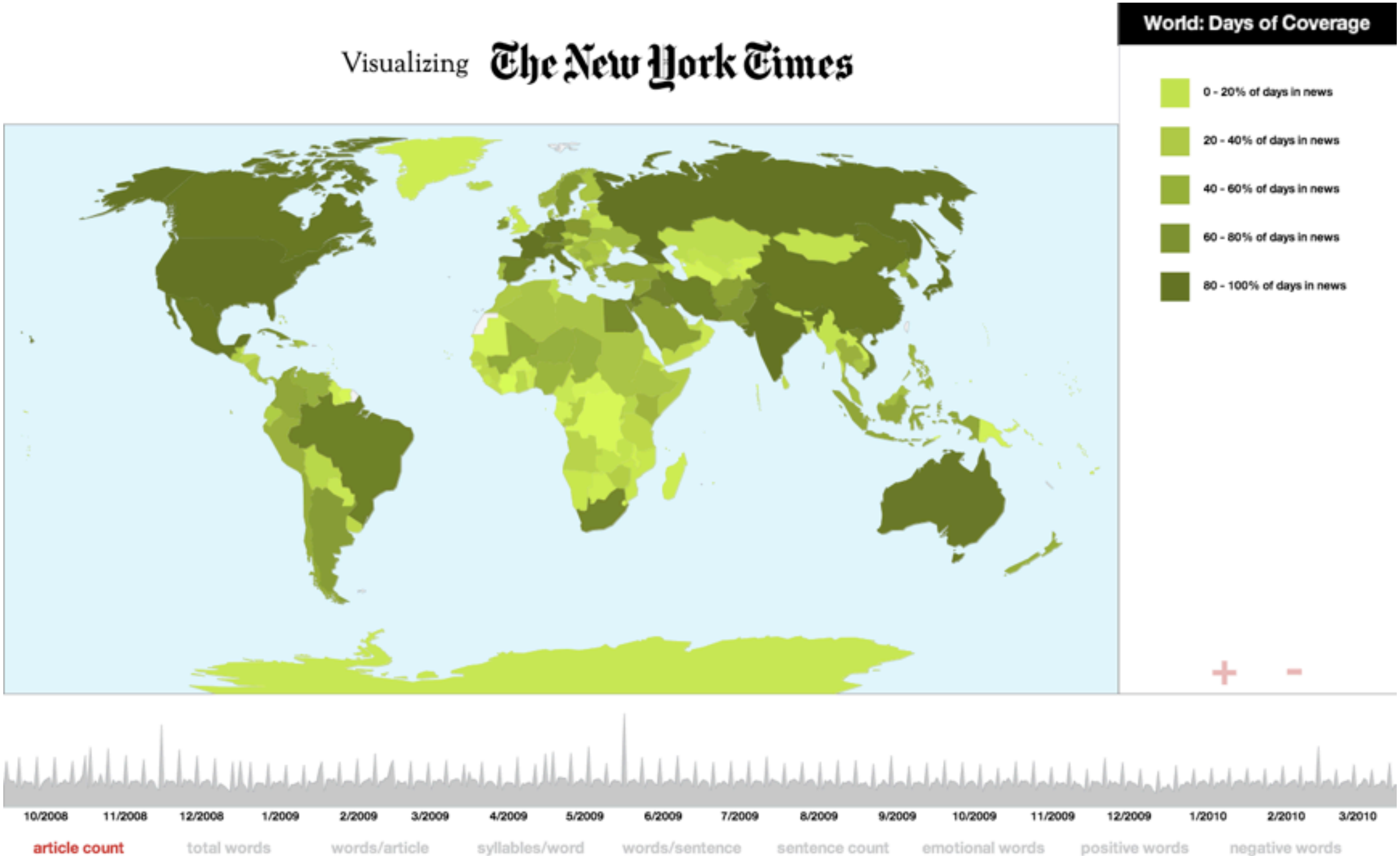

Visualizing The New York Times
World: Days of Coverage
0 - 20% of days in news
20 - 40% of days in news
40 - 60% of days in news
60 - 80% of days in news
80 - 100% of days in news
+
-
10/2008
11/2008
12/2008
1/2009
2/2009
3/2009
4/2009
5/2009
6/2009
7/2009
8/2009
9/2009
10/2009
11/2009
12/2009
1/2010
2/2010
3/2010
article count
total words
words/article
syllables/word
words/sentence
sentence count
emotional words
positive words
negative words

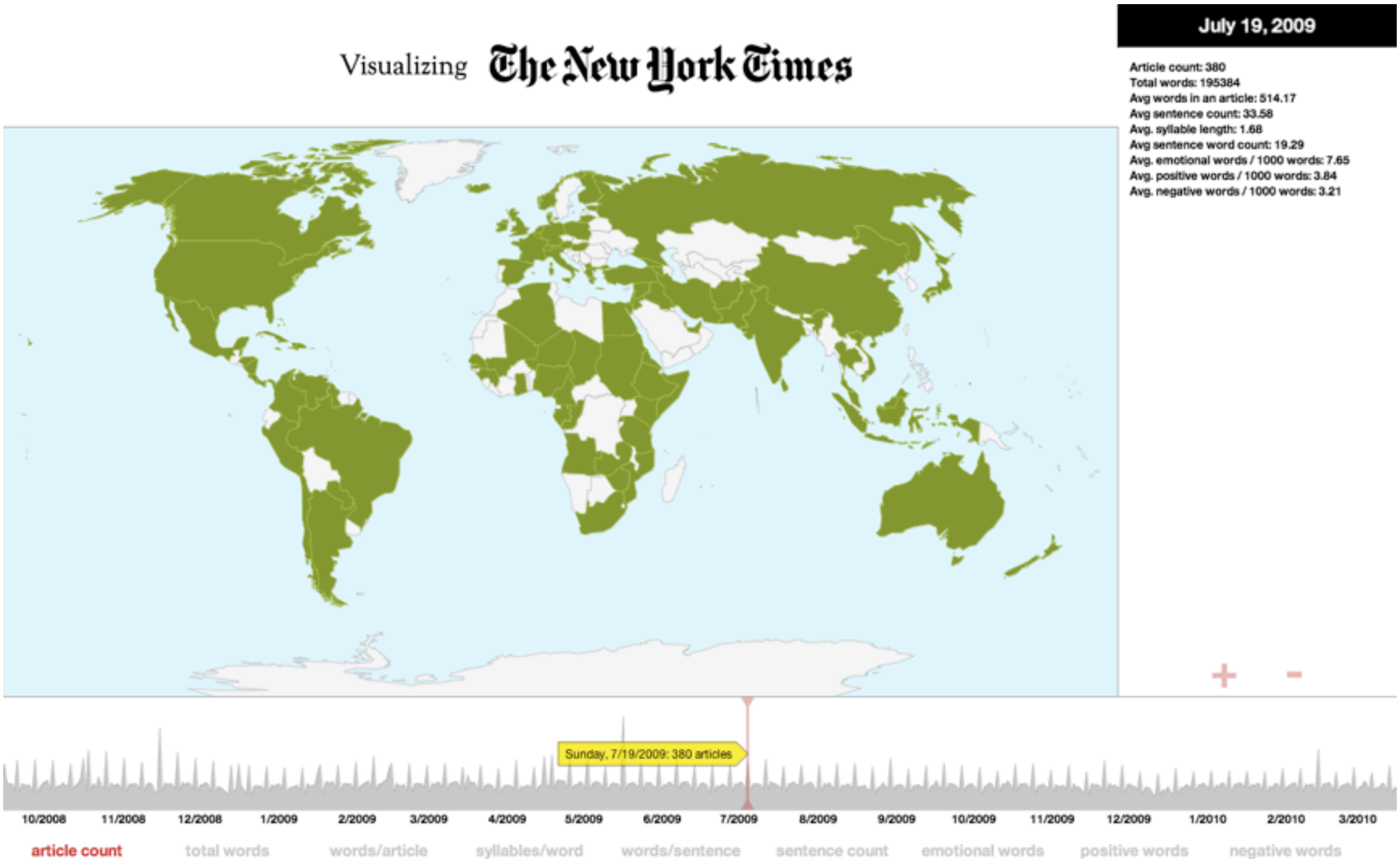
Visualizing The New York Times
July 19, 2009
Article count: 380
Total words: 195384
Avg words in an article: 514.17
Avg sentence count: 33.58
Avg. syllable length: 1.68
Avg sentence word count: 19.29
Avg. emotional words / 1000 words: 7.65
Avg. positive words / 1000 words: 3.84
Avg. negative words / 1000 words: 3.21
+
-
Sunday, 7/19/2009: 380 articles
10/2008
11/2008
12/2008
1/2009
2/2009
3/2009
4/2009
5/2009
6/2009
7/2009
8/2009
9/2009
10/2009
11/2009
12/2009
1/2010
2/2010
3/2010
article count
total words
words/article
syllables/word
words/sentence
sentence count
emotional words
positive words
negative words

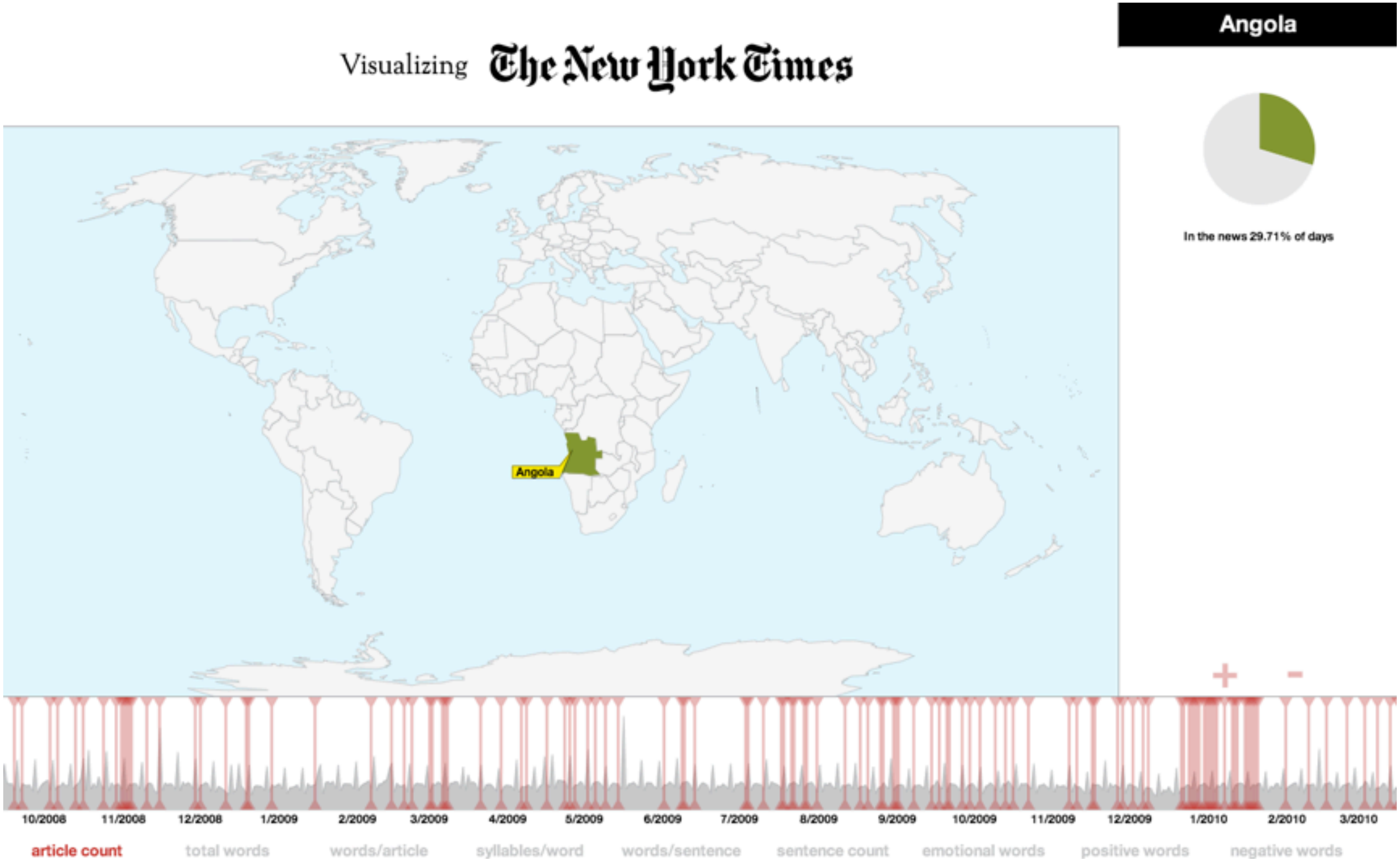

Visualizing The New York Times
Angola
In the news 29.71% of days
Angola
+
-
10/2008
11/2008
12/2008
1/2009
2/2009
3/2009
4/2009
5/2009
6/2009
7/2009
8/2009
9/2009
10/2009
11/2009
12/2009
1/2010
2/2010
3/2010
article count
total words
words/article
syllables/word
words/sentence
sentence count
emotional words
positive words
negative words


"All the News That's Fit to Print"

The New York Times

Late Edition

NEW YORK, TUESDAY, DECEMBER 18, 2007

Fed and Regulators Shrugged As the Subprime Crisis Spread

Analysis Finds Trail of Warnings on Loans

Radio to Link Police in State Fails First Test

For Romney, a Course Set Long Ago

RUSSIA DELIVERS ITS NUCLEAR FUEL TO PLANT IN IRAN

A SETBACK FOR THE U.S.

Moscow Cites Controls on Supply — Second Plant Is Planned

With Regrets, New Orleans

***geo**tag*



Draft version October 18, 2010
Preprint typeset using LaTeX style emulateapj v. 11/10/09

INVESTIGATING THE COSMIC-RAY IONIZATION RATE NEAR THE SUPERNOVA REMNANT IC 443 THROUGH $H_3^+$ OBSERVATIONS[1,2]

Nick Indriolo[3], Geoffrey A. Blake[4], Miwa Goto[5], Tomonori Usuda[6], Takeshi Oka[7], T. R. Geballe[8], Brian D. Fields[3,9] Benjamin J. McCall[3,9,10]

*Draft version October 18, 2010*

ABSTRACT

Observational and theoretical evidence suggests that high-energy Galactic cosmic rays are primarily accelerated by supernova remnants. If also true for low-energy cosmic rays, the ionization rate near a supernova remnant should be higher than in the general Galactic interstellar medium (ISM). We have searched for $H_3^+$ absorption features in 6 sight lines which pass through molecular material near IC 443—a well-studied case of a supernova remnant interacting with its surrounding molecular material—for the purpose of inferring the cosmic-ray ionization rate in the region. In 2 of the sight lines (toward ALS 8828 and HD 254577) we find large $H_3^+$ column densities, $N(H_3^+) \approx 3 \times 10^{14}$ cm$^{-2}$, and deduce ionization rates of $\zeta_2 \approx 2 \times 10^{-15}$ s$^{-1}$, about 5 times larger than inferred toward average diffuse molecular cloud sight lines. However, the $3\sigma$ upper limits found for the other 4 sight lines are consistent with typical Galactic values. This wide range of ionization rates is likely the result of particle acceleration and propagation effects, which predict that the cosmic-ray spectrum and thus ionization rate should vary in and around the remnant. While we cannot determine if the $H_3^+$ absorption arises in post-shock (interior) or pre-shock (exterior) gas, the large inferred ionization rates suggest that IC 443 is in fact accelerating a large population of low-energy cosmic rays. Still, it is unclear whether this population can propagate far enough into the ISM to account for the ionization rate inferred in diffuse Galactic sight lines.

*Subject headings:* astrochemistry – cosmic rays – ISM: supernova remnants

1. INTRODUCTION

As cosmic rays propagate through the interstellar medium (ISM) they interact with the ambient material. These interactions include excitation and ionization of atoms and molecules, spallation of nuclei, excitation of nuclear states, and the production of neutral pions ($\pi^0$) which decay into gamma-rays. Evidence suggests that Galactic cosmic rays are primarily accelerated by supernova remnants (SNRs) through the process of diffusive shock acceleration (e.g. Drury 1983; Blandford & Eichler 1987), so interstellar clouds in close proximity to an SNR should provide a prime "laboratory" for studying these interactions. IC 443 represents such a case, as portions of the SNR shock are known to be interacting with the neighboring molecular clouds.

IC 443 is an intermediate age remnant (about 30,000 yr; Chevalier 1999) located in the Galactic anti-center region $(l, b) \approx (189°, +3°)$ at a distance of about 1.5 kpc in the Gem OB1 association (Welsh & Sallmen 2003), and is a particularly well-studied SNR. Figure 1 shows the red image of IC 443 taken during the Second Palomar Observatory Sky Survey. The remnant is composed of subshells A and B; shell A is to the NE—its center at $\alpha = 06^h17^m08.4^s$, $\delta = +22°36'39.4''$ J2000.0 is marked by the cross—while shell B is to the SW. Adopting a distance of 1.5 kpc, the radii of subshells A and B are about 7 pc and 11 pc, respectively. Between the subshells is a darker lane that runs across the remnant from the NW to SE. This is a molecular cloud which has been mapped in $^{12}$CO emission (Cornett et al. 1977; Dickman et al. 1992; Zhang et al. 2009), and is known to be in the foreground because it absorbs X-rays emitted by the hot remnant interior (Troja et al. 2006). Aside from this quiescent foreground cloud, observations of the $J = 1 \rightarrow 0$ line of $^{12}$CO also show shocked molecular material coincident with IC 443 (DeNoyer 1979; Huang et al. 1986; Dickman et al. 1992; Wang & Scoville 1992). These shocked molecular clumps first identified by DeNoyer (1979) and Huang et al. (1986) in CO have also been observed in several atomic and small molecular species (e.g. White et al. 1987; Burton et al. 1988; van Dishoeck et al. 1993; White 1994; Snell et al. 2005), and are thought to be the result of the expanding SNR interacting with the surrounding ISM. While many of the shocked clumps are coincident with the quiescent gas, it

[1] Some of the data presented herein were obtained at the W.M. Keck Observatory, which is operated as a scientific partnership among the California Institute of Technology, the University of California and the National Aeronautics and Space Administration. The Observatory was made possible by the generous financial support of the W.M. Keck Foundation.
[2] Based in part on data collected at Subaru Telescope, which is operated by the National Astronomical Observatory of Japan.
[3] Department of Astronomy, University of Illinois at Urbana-Champaign, Urbana, IL 61801
[4] Division of Geological and Planetary Sciences and Division of Chemistry and Chemical Engineering, MS 150-21, California Institute of Technology, Pasadena, CA 91125
[5] Max-Planck-Institut für Astronomie, Königstuhl 17, Heidelberg D-69117, Germany
[6] Subaru Telescope, 650 North A'ohoku Place, Hilo, HI 96720
[7] Department of Astronomy and Astrophysics and Department of Chemistry, University of Chicago, Chicago, IL 60637
[8] Gemini Observatory, 670 North A'ohoku Place, Hilo, HI 96720
[9] Department of Physics, University of Illinois at Urbana-Champaign, Urbana, IL 61801
[10] Department of Chemistry, University of Illinois at Urbana-Champaign, Urbana, IL 61801

***astro**tag*

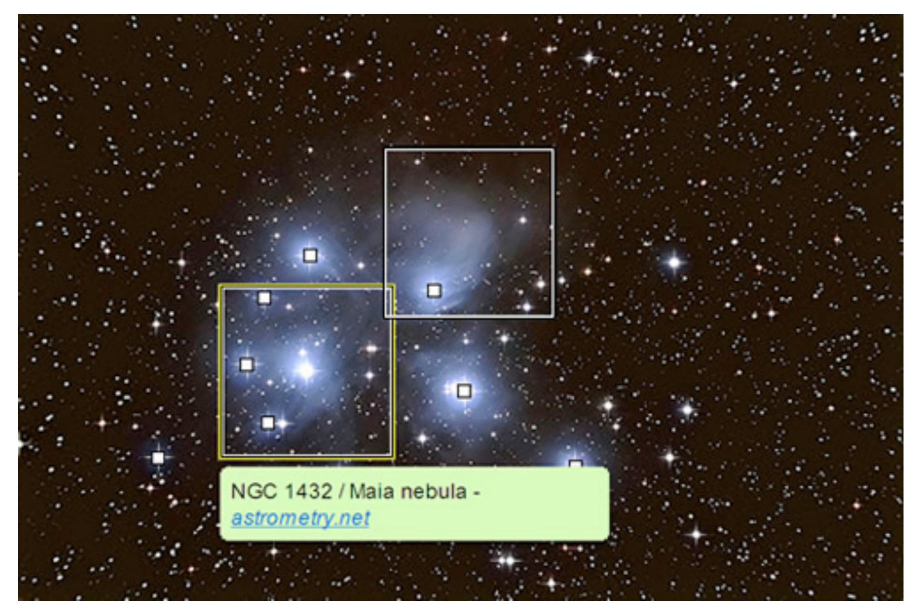

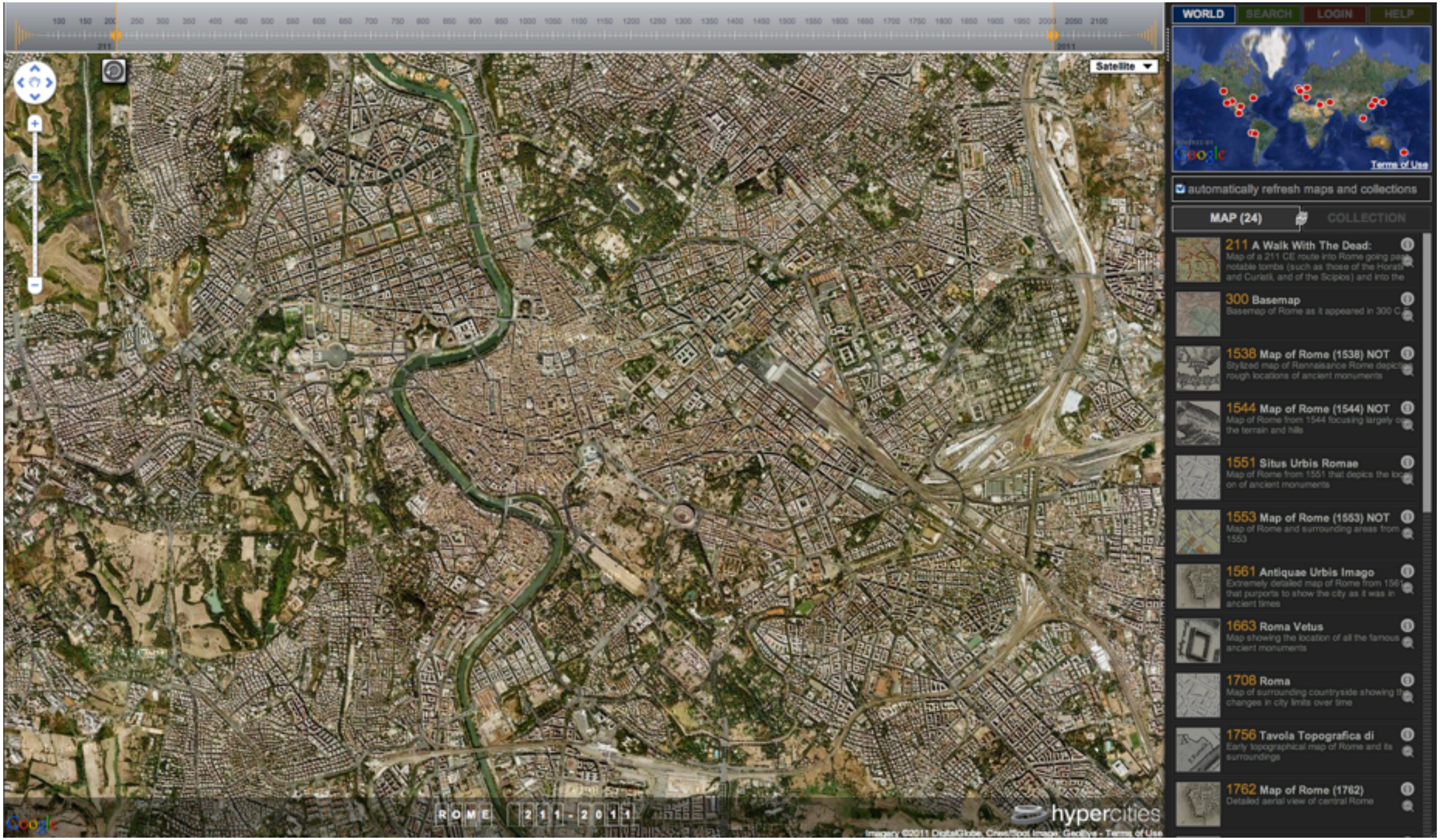
WORLD
SEARCH
LOGIN
HELP
Satellite
automatically refresh maps and collections
MAP (24)
COLLECTION
211 A Walk With The Dead:
Map of a 211 CE route into Rome going
notable tombs (such as those of the Horatii
and Curiatii, and of the Scipios) and into the
300 Basemap
Basemap of Rome as it appeared in 300 C
1538 Map of Rome (1538) NOT
Stylized map of Rennaisance Rome
rough locations of ancient monuments
1544 Map of Rome (1544) NOT
Map of Rome from 1544 focusing largely
the terrain and hills
1551 Situs Urbis Romae
Map of Rome from 1551 that depics the
on of ancient monuments
1553 Map of Rome (1553) NOT
Map of Rome and surrounding areas from
1553
1561 Antiquae Urbis Imago
Extremely detailed map of Rome from 1561
that purports to show the city as it was in
ancient times
1663 Roma Vetus
Map showing the location of all the famous
ancient monuments
1708 Roma
Map of surrounding countryside showing
changes in city limits over time
1756 Tavola Topografica di
Early topographical map of Rome and its
surroundings
1762 Map of Rome (1762)
Detailed aerial view of central Rome
ROME
211-2011
hypercities
Imagery ©2011 DigitalGlobe, Cnes/Spot Image, GeoEye - Terms of Use

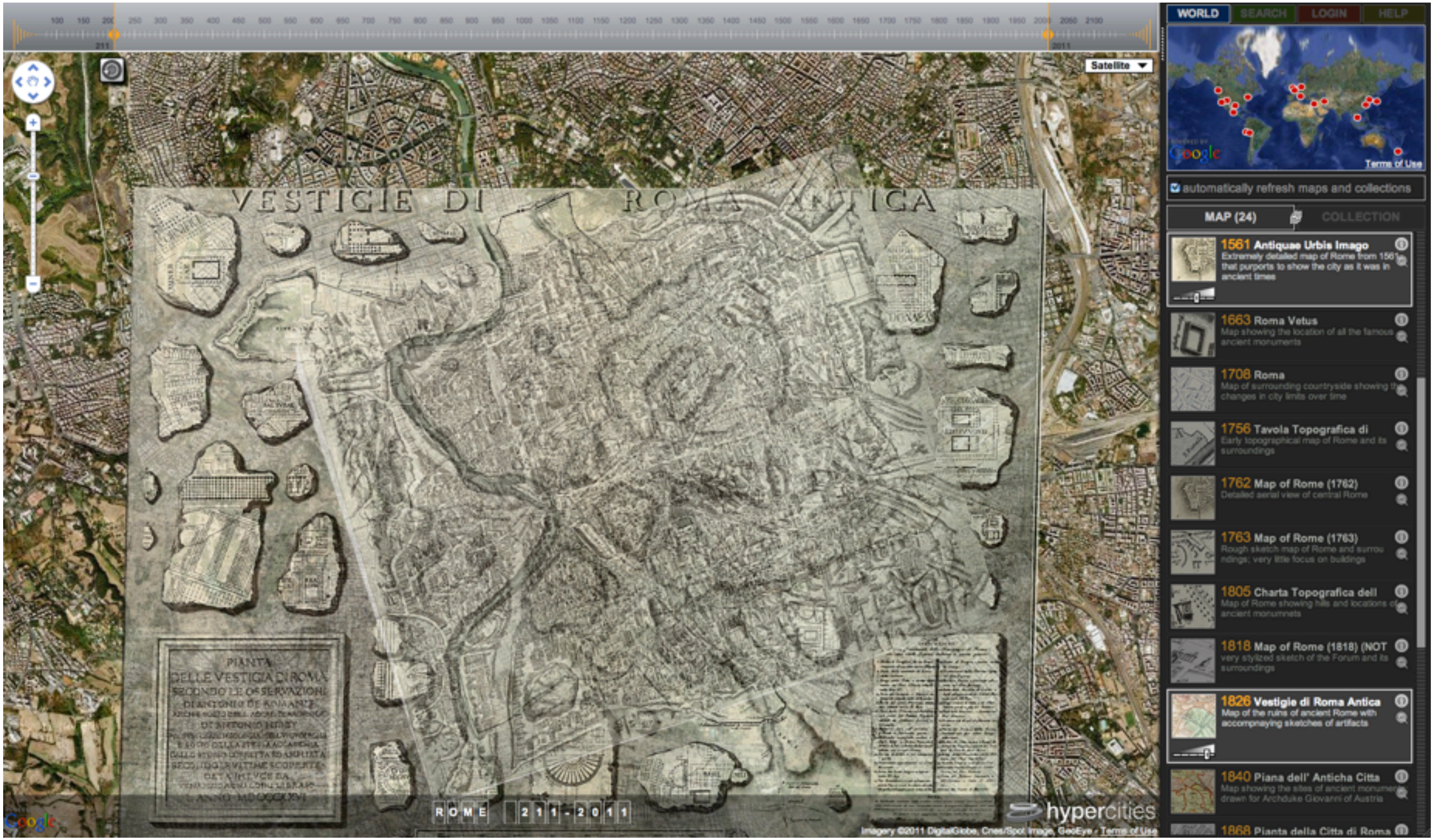

WORLD
SEARCH
LOGIN
HELP
automatically refresh maps and collections
MAP (24)
COLLECTION
1561 Antiquae Urbis Imago
Extremely detailed map of Rome from 1561 that purports to show the city as it was in ancient times
1663 Roma Vetus
Map showing the location of all the famous ancient monuments
1708 Roma
Map of surrounding countryside showing the changes in city limits over time
1756 Tavola Topografica di
Early topographical map of Rome and its surroundings
1762 Map of Rome (1762)
Detailed aerial view of central Rome
1763 Map of Rome (1763)
Rough sketch map of Rome and surroundings; very little focus on buildings
1805 Charta Topografica dell
Map of Rome showing hills and locations of ancient monumnets
1818 Map of Rome (1818) (NOT
very stylized sketch of the Forum and its surroundings
1826 Vestigie di Roma Antica
Map of the ruins of ancient Rome with accompnaying sketches of artifacts
1840 Piana dell' Anticha Citta
Map showing the sites of ancient monuments drawn for Archduke Giovanni of Austria
1868 Pianta della Citta di Roma
Satellite
VESTIGIE DI ROMA ANTICA
ROME
211 - 2011
hypercities

***geo**reference*


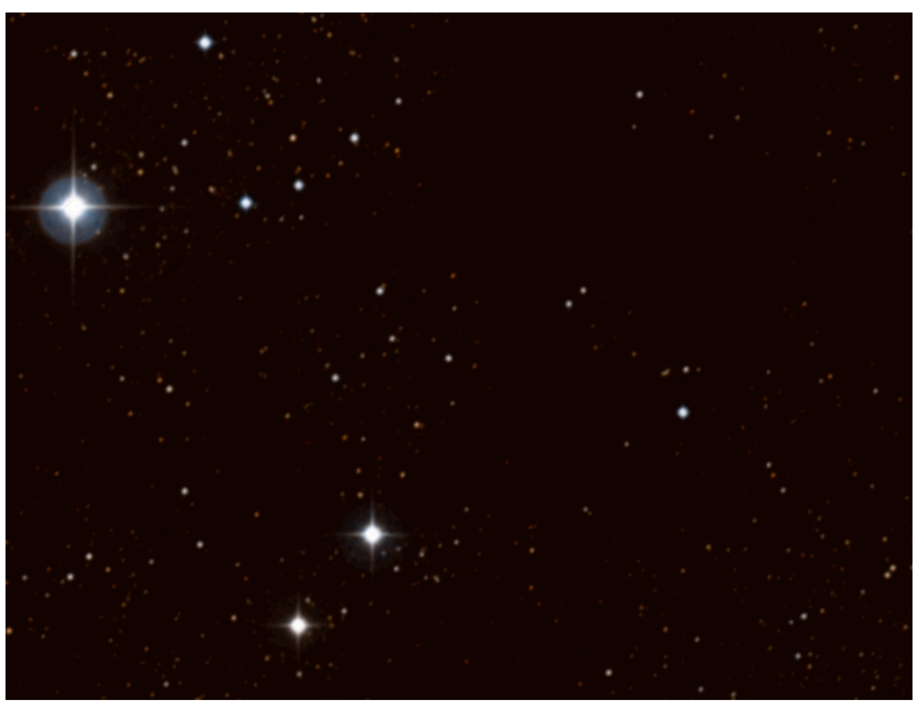

***astro**reference*

Draft version October 18, 2010
Preprint typeset using LaTeX style emulateapj v. 11/10/09

# INVESTIGATING THE COSMIC-RAY IONIZATION RATE NEAR THE SUPERNOVA REMNANT IC 443 THROUGH $H_3^+$ OBSERVATIONS[1,2]

Nick Indriolo[3], Geoffrey A. Blake[4], Miwa Goto[5], Tomonori Usuda[6], Takeshi Oka[7], T. R. Geballe[8], Brian D. Fields[3,9] Benjamin J. McCall[3,9,10]

*Draft version October 18, 2010*

## ABSTRACT

Observational and theoretical evidence suggests that high-energy Galactic cosmic rays are primarily accelerated by supernova remnants. If also true for low-energy cosmic rays, the ionization rate near a supernova remnant should be higher than in the general Galactic interstellar medium (ISM). We have searched for $H_3^+$ absorption features in 6 sight lines which pass through molecular material near IC 443—a well-studied case of a supernova remnant interacting with its surrounding molecular material—for the purpose of inferring the cosmic-ray ionization rate in the region. In 2 of the sight lines (toward ALS 8828 and HD 254577) we find large $H_3^+$ column densities, $N(H_3^+) \approx 3 \times 10^{14}$ cm$^{-2}$, and deduce ionization rates of $\zeta_2 \approx 2 \times 10^{-15}$ s$^{-1}$, about 5 times larger than inferred toward average diffuse molecular cloud sight lines. However, the $3\sigma$ upper limits found for the other 4 sight lines are consistent with typical Galactic values. This wide range of ionization rates is likely the result of particle acceleration and propagation effects, which predict that the cosmic-ray spectrum and thus ionization rate should vary in and around the remnant. While we cannot determine if the $H_3^+$ absorption arises in post-shock (interior) or pre-shock (exterior) gas, the large inferred ionization rates suggest that IC 443 is in fact accelerating a large population of low-energy cosmic rays. Still, it is unclear whether this population can propagate far enough into the ISM to account for the ionization rate inferred in diffuse Galactic sight lines.

*Subject headings:* astrochemistry – cosmic rays – ISM: supernova remnants

## 1. INTRODUCTION

As cosmic rays propagate through the interstellar medium (ISM) they interact with the ambient material. These interactions include excitation and ionization of atoms and molecules, spallation of nuclei, excitation of nuclear states, and the production of neutral pions ($\pi^0$) which decay into gamma-rays. Evidence suggests that Galactic cosmic rays are primarily accelerated by supernova remnants (SNRs) through the process of diffusive shock acceleration (e.g. Drury 1983; Blandford & Eichler 1987), so interstellar clouds in close proximity to an SNR should provide a prime "laboratory" for studying these interactions. IC 443 represents such a case, as portions of the SNR shock are known to be interacting with the neighboring molecular clouds.

IC 443 is an intermediate age remnant (about 30,000 yr; Chevalier 1999) located in the Galactic anti-center region $(l, b) \approx (189°, +3°)$ at a distance of about 1.5 kpc in the Gem OB1 association (Welsh & Sallmen 2003), and is a particularly well-studied SNR. Figure 1 shows the red image of IC 443 taken during the Second Palomar Observatory Sky Survey. The remnant is composed of subshells A and B; shell A is to the NE—its center at $\alpha = 06^h17^m08.4^s$, $\delta = +22°36'39.4''$ J2000.0 is marked by the cross—while shell B is to the SW. Adopting a distance of 1.5 kpc, the radii of subshells A and B are about 7 pc and 11 pc, respectively. Between the subshells is a darker lane that runs across the remnant from the NW to SE. This is a molecular cloud which has been mapped in $^{12}$CO emission (Cornett et al. 1977; Dickman et al. 1992; Zhang et al. 2009), and is known to be in the foreground because it absorbs X-rays emitted by the hot remnant interior (Troja et al. 2006). Aside from this quiescent foreground cloud, observations of the $J = 1 \rightarrow 0$ line of $^{12}$CO also show shocked molecular material coincident with IC 443 (DeNoyer 1979; Huang et al. 1986; Dickman et al. 1992; Wang & Scoville 1992). These shocked molecular clumps first identified by DeNoyer (1979) and Huang et al. (1986) in CO have also been observed in several atomic and small molecular species (e.g. White et al. 1987; Burton et al. 1988; van Dishoeck et al. 1993; White 1994; Snell et al. 2005), and are thought to be the result of the expanding SNR interacting with the surrounding ISM. While many of the shocked clumps are coincident with the quiescent gas, it

[1] Some of the data presented herein were obtained at the W.M. Keck Observatory, which is operated as a scientific partnership among the California Institute of Technology, the University of California and the National Aeronautics and Space Administration. The Observatory was made possible by the generous financial support of the W.M. Keck Foundation.
[2] Based in part on data collected at Subaru Telescope, which is operated by the National Astronomical Observatory of Japan.
[3] Department of Astronomy, University of Illinois at Urbana-Champaign, Urbana, IL 61801
[4] Division of Geological and Planetary Sciences and Division of Chemistry and Chemical Engineering, MS 150-21, California Institute of Technology, Pasadena, CA 91125
[5] Max-Planck-Institut für Astronomie, Königstuhl 17, Heidelberg D-69117, Germany
[6] Subaru Telescope, 650 North A'ohoku Place, Hilo, HI 96720
[7] Department of Astronomy and Astrophysics and Department of Chemistry, University of Chicago, Chicago, IL 60637
[8] Gemini Observatory, 670 North A'ohoku Place, Hilo, HI 96720
[9] Department of Physics, University of Illinois at Urbana-Champaign, Urbana, IL 61801
[10] Department of Chemistry, University of Illinois at Urbana-Champaign, Urbana, IL 61801

| N | Identifier | Otype | ICRS (J2000) RA | ICRS (J2000) DEC | Sp type | #ref 1850 - 2011 | #notes |
|---|---|---|---|---|---|---|---|
| 1 | * zet Per | V* | 03 54 07.9215 | +31 53 01.088 | B1Ib | 706 | 1 |
| 2 | CCDM J03554+3103A | ** | 03 55 23.0773 | +31 02 45.014 | O9.5IIIe-B0Ve | 720 | 0 |
| 3 | NAME ELNATH | *i* | 05 26 17.5134 | +28 36 26.820 | B7III | 287 | 1 |
| 4 | * zet Tau | Be* | 05 37 38.6858 | +21 08 33.177 | B2IV | 592 | 0 |
| 5 | Ass Gem OB 1- | As* | 06 09.8 | +21 35 | ~ | 118 | 0 |
| 6 | TYC 1877-287-1 | * | 06 16 13.3409 | +22 45 48.634 | sdO | 9 | 0 |
| 7 | HD 254577 | * | 06 17 54.3853 | +22 24 32.928 | B0.5II-III | 30 | 0 |
| 8 | HD 43582 | V* | 06 18 00.3459 | +22 39 29.995 | B0IIIn | 21 | 0 |
| 9 | IC 443 | SNR | 06 18 02.7 | +22 39 36 | S | 729 | 2 |
| 10 | HD 254755 | * | 06 18 31.7741 | +22 40 45.125 | O9Vp | 33 | 0 |


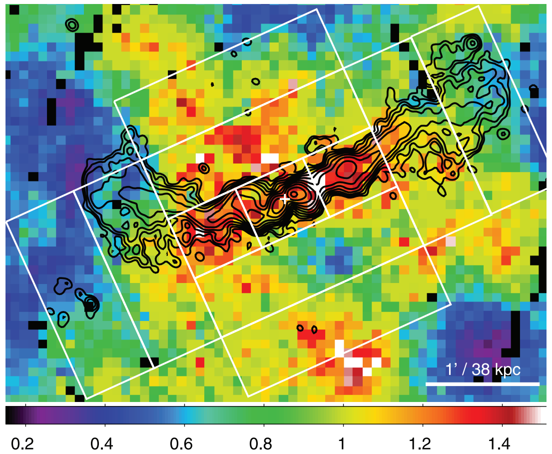


**Figure 3.** Abundance map of the core of AWM 4, with GMRT 610-MI contours overlaid. Rectangular regions were used to examine the variati in abundance across and along the jet. The white cross marks the positi of the radio core.

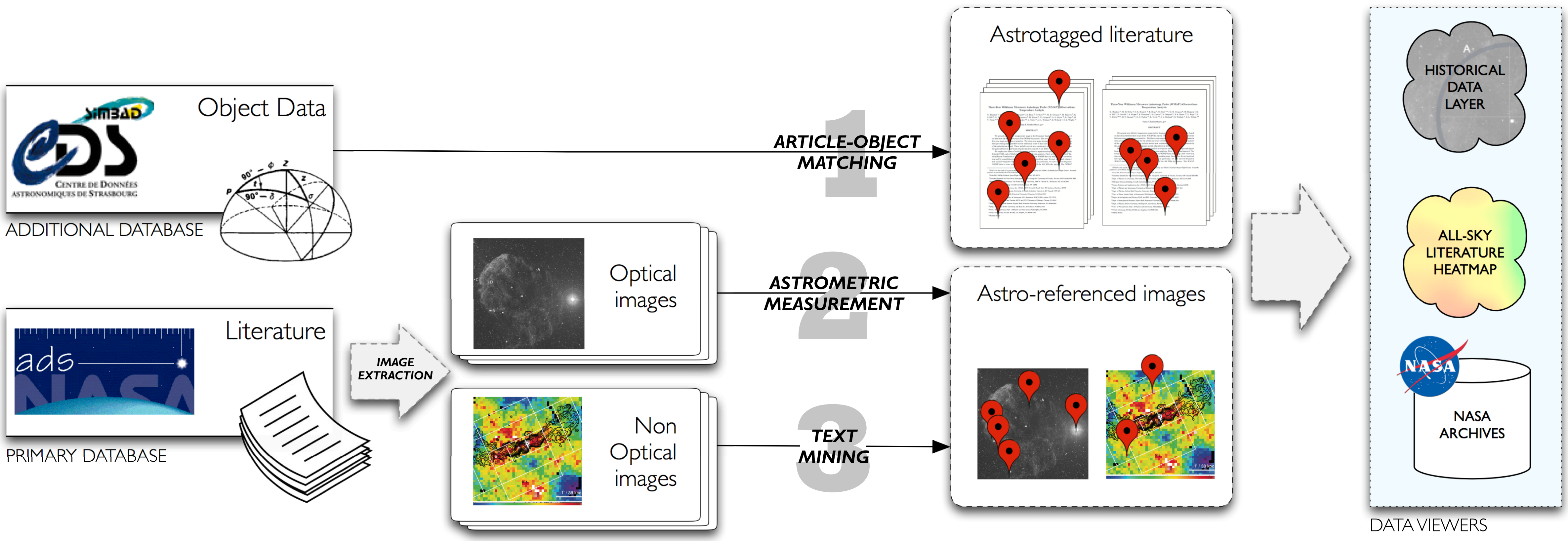

Object Data
SIMBAD
CDS
CENTRE DE DONNÉES ASTRONOMIQUES DE STRASBOURG
ADDITIONAL DATABASE
Literature
ads
NASA
PRIMARY DATABASE
IMAGE EXTRACTION
Optical images
Non Optical images
1
ARTICLE-OBJECT MATCHING
2
ASTROMETRIC MEASUREMENT
3
TEXT MINING
Astrotagged literature
Astro-referenced images
HISTORICAL DATA LAYER
ALL-SKY LITERATURE HEATMAP
NASA
NASA ARCHIVES
DATA VIEWERS

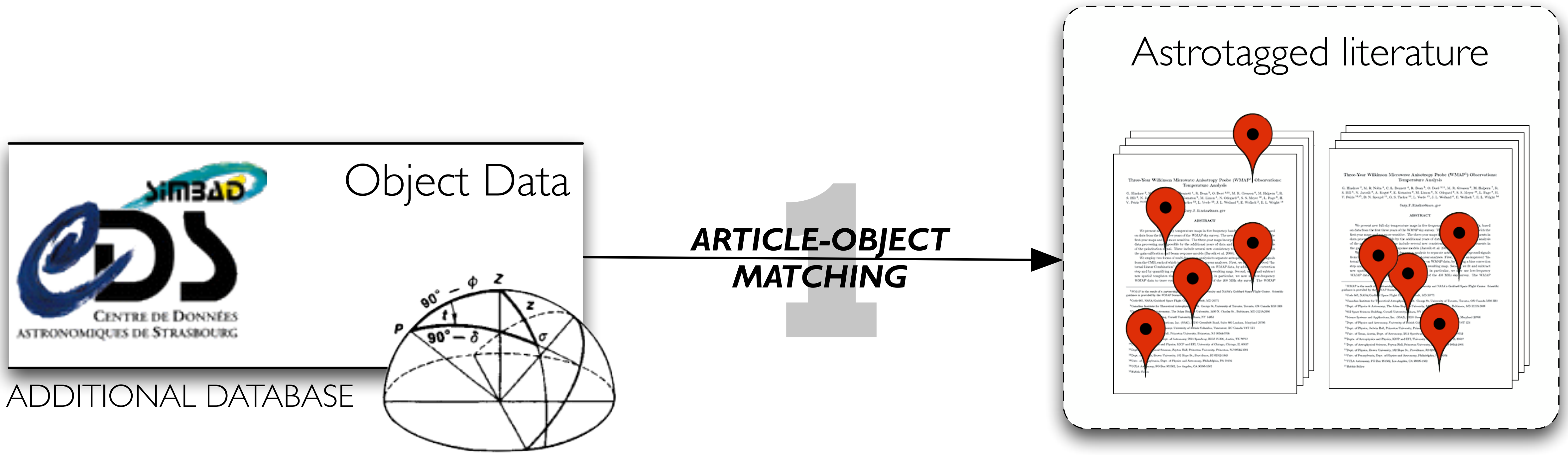

Object Data
SIMBAD
CENTRE DE DONNÉES
ASTRONOMIQUES DE STRASBOURG
ADDITIONAL DATABASE
1
ARTICLE-OBJECT
MATCHING
Astrotagged literature


An **astrotag** consists of an ADS paper (bibcode) linked to either an object (RA, DEC) or a tile in a Healpix map

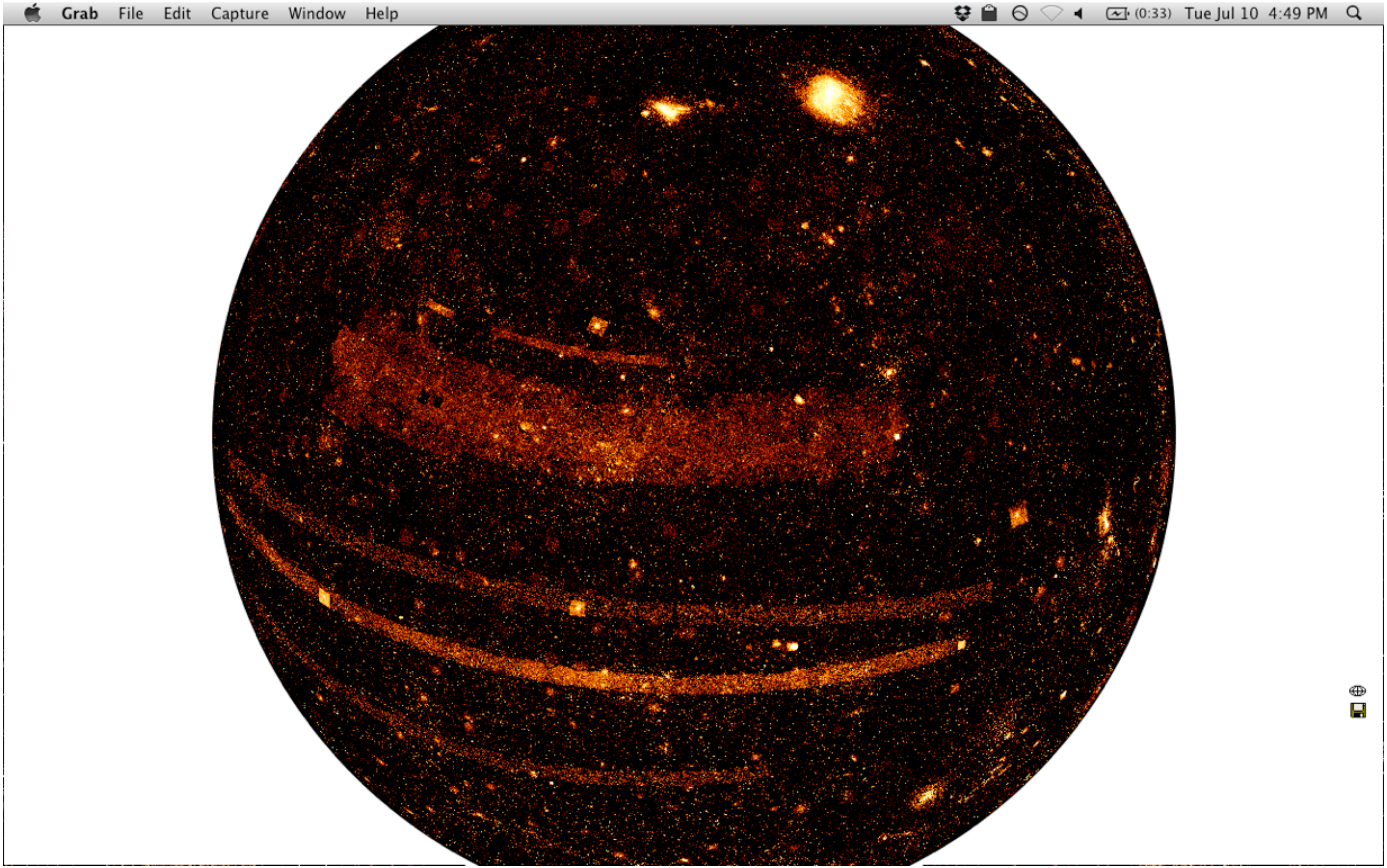
Grab File Edit Capture Window Help
(0:33) Tue Jul 10 4:49 PM

author:"^Goodman, A" – Most cited – NASA ADS

http://labs.adsabs.harvard.edu/ui/cgi-bin/topicSearch?q=+author%3A

# ADS Labs
## Streamlined Search

Home | Labs Home | ADS Classic | Help | Sign on

**author:"^Goodman, A" - *Most cited*** *27 results* More

Dates: Min_1992 [X] AND Max_2005 [X] clear

**FILTER BY:**

- Authors
- Keywords
- Data
- SIMBAD Objects
  - Other object (12)
  - Star (7)
  - Infrared Source (2)
  - Galaxy (1)
    - M 31 (1)
    - NGC 4038 (1)
    - NGC 4039 (1)
  - Radio Source (1)
- Vizier Tables
- Refereed status
- Dates

from 1992 to 2005

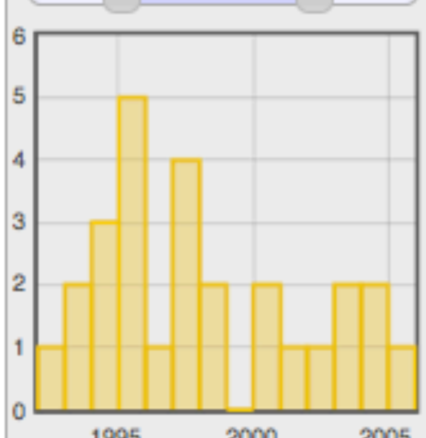


1. 1993ApJ...406..528G **Dense cores in dark clouds. VIII - Velocity gradients**
Goodman, A. A.; Benson, P. J.; Fuller, G. A.; Myers, P. C.
*Astrophysical Journal, Part 1 (ISSN 0004-637X), vol. 406, no. 2, p. 528-547. Apr 1993*

2. 1998ApJ...504..223G **Coherence in Dense Cores. II. The Transition to Coherence**
Goodman, Alyssa A.; Barranco, Joseph A.; Wilner, David J.; Heyer, Mark H.
*Astrophysical Journal v.504, p.223 Sep 1998*

4. 1995ApJ...448..748G **Does Near-Infrared Polarimetry Reveal the Magnetic Field in Cold Dark Clouds?**
Goodman, Alyssa A.; Jones, Terry J.; Lada, Elizabeth A.; Myers, Philip C.
*Astrophysical Journal v.448, p.748 Aug 1995*

7. 1992ApJ...399..108G **The structure of magnetic fields in dark clouds - Infrared polarimetry in B216-217**
Goodman, Alyssa A.; Jones, Terry J.; Lada, Elizabeth A.; Myers, Philip C.
*Astrophysical Journal, Part 1 (ISSN 0004-637X), vol. 399, no. 1, p. 108-113. Nov 1992*

8. 1995ApJ...455L.181G **A Point in Favor of the Superparamagnetic Grain Hypothesis**
Goodman, A. A.; Whittet, D. C. B.
*Astrophysical Journal Letters v.455, p.L181 Dec 1995*

9. 1994ApJ...424..208G **The magnetic field in the Ophiuchus dark cloud complex**
Goodman, Alyssa A.; Heiles, Carl
*Astrophysical Journal, Part 1 (ISSN 0004-637X), vol. 424, no. 1, p. 208-221 Mar 1994*

11. 1996ASPC...97..325G **The Interpretation of Polarization Position Angle Measurements**
Goodman, A. A.
*Polarimetry of the interstellar medium. Astronomical Society of the Pacific Conference Series; Vol. 97; Proceedings of a conference held at Rensselaer Polytechnic Institute; Troy; New York; 4-7 June 1995; San Francisco: Astronomical Society of the Pacific (ASP); lc1996; edited by Wayne G. Roberge and Doug C. B. Whittet, p.325 n/a 1996*

12. 2004ApJ...608..831G **PV Cephei: Young Star Caught Speeding?**
Goodman, Alyssa A.; Arce, Héctor G.
*The Astrophysical Journal, Volume 608, Issue 2, pp. 831-845. Jun 2004*

13. 1995ASPC...73...45G **The future of magnetic field mapping in the Interstellar Medium**
Goodman, Alyssa A.
*In Astronomical Society of the Pacific, Airborne Astronomy Symposium on the Galactic Ecosystem: From Gas to Stars to Dust, Volume 73 p 45-52 (SEE N96-13618 02-88) n/a 1995*

14. 2004ASPC..323..171G **The COMPLETE Survey of Star-Forming Regions on its Second Birthday**
Goodman, A. A.

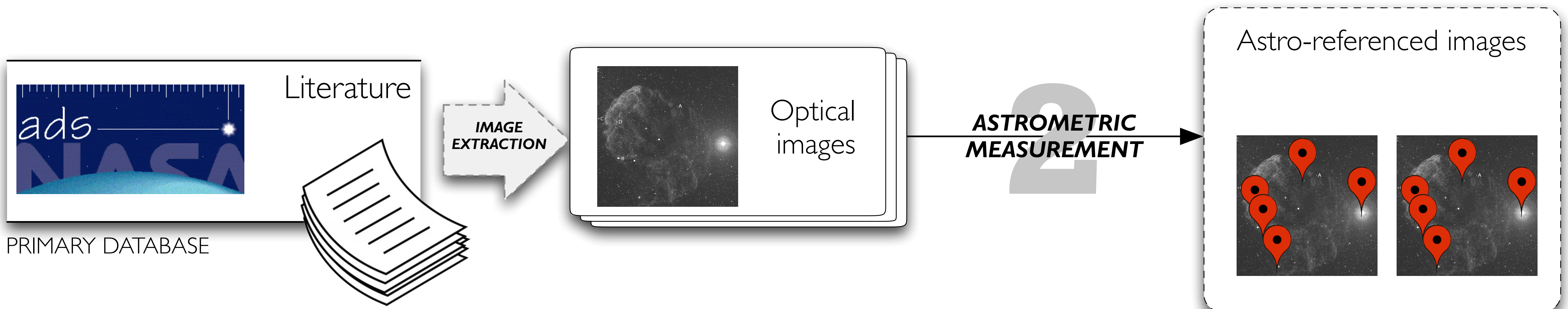
Literature
PRIMARY DATABASE
IMAGE EXTRACTION
Optical images
ASTROMETRIC MEASUREMENT
2
Astro-referenced images

An **astroreference** consists of coordinates, orientation and pixel scale of an image, e.g.

astrometry.net (2 weeks ago)
Hello, this is the blind astrometry solver. Your results are:
(RA, Dec) center:(290.237430258, 11.1399605323) degrees
(RA, Dec) center (H:M:S, D:M:S):(19:20:56.983, +11:08:23.858)
Orientation:89.92 deg E of N

Pixel scale:1.11 arcsec/pixel

Parity:Reverse ("Left-handed")
Field size :38.69 x 20.67 arcminutes

View in World Wide Telescope

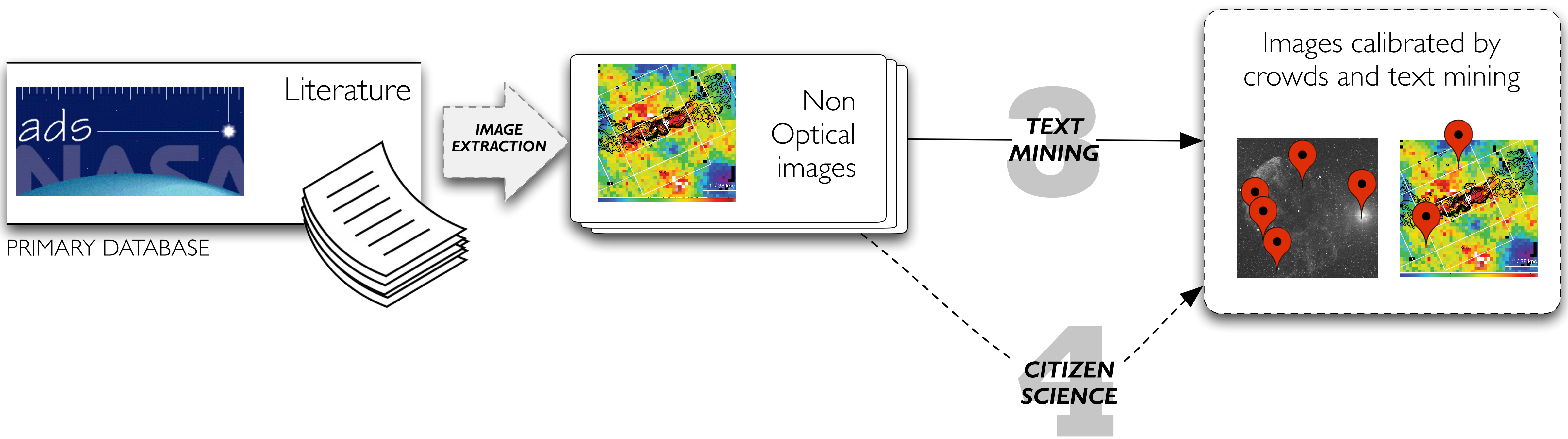
Literature
ads
NASA
PRIMARY DATABASE
IMAGE EXTRACTION
Non Optical images
3
TEXT MINING
4
CITIZEN SCIENCE
Images calibrated by crowds and text mining

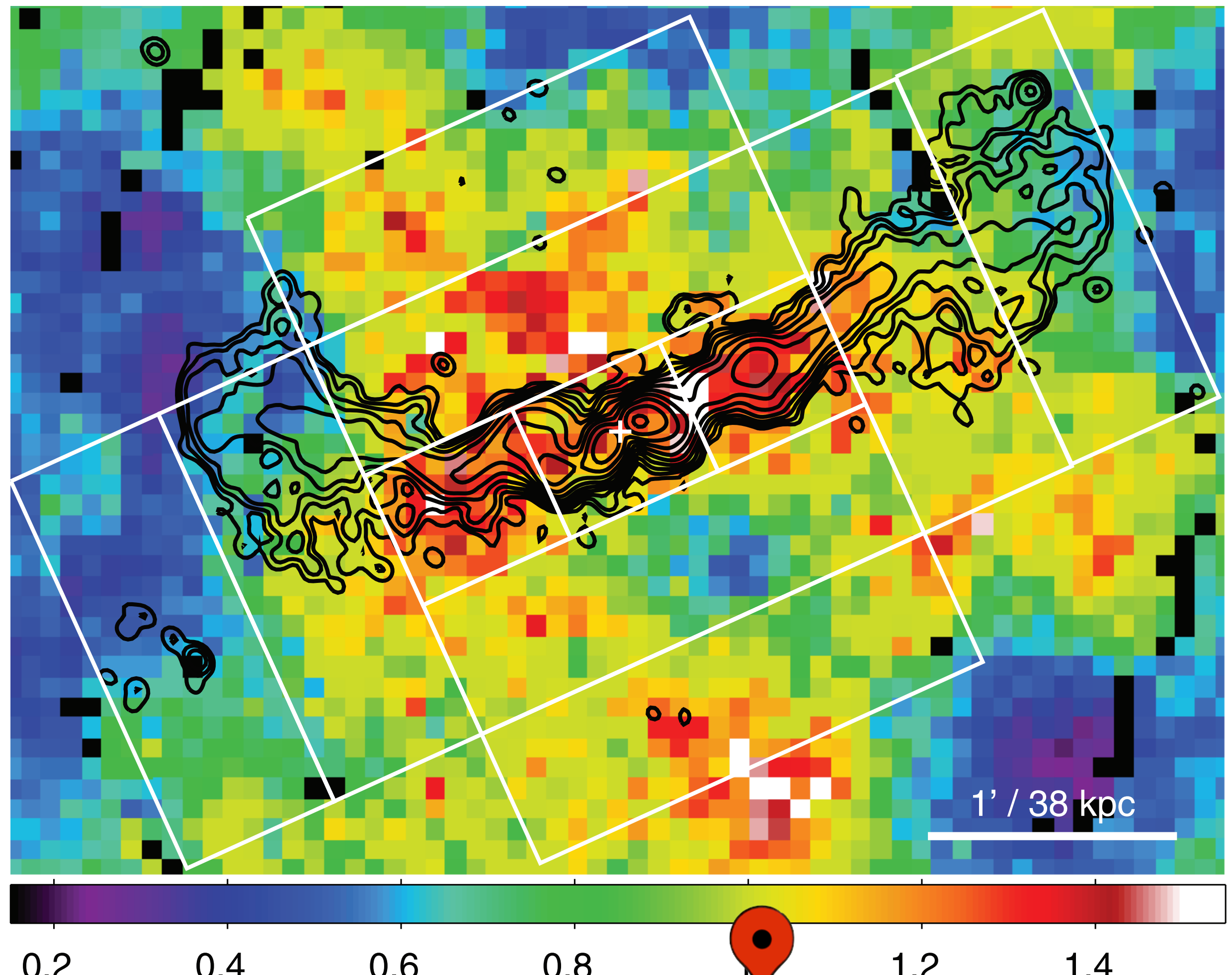


**Figure 3.** Abundance map of the core of AWM 4, with GMRT 610-MHz contours overlaid. Rectangular regions were used to examine the variation in abundance across and along the jet. The white cross marks the position of the radio core.

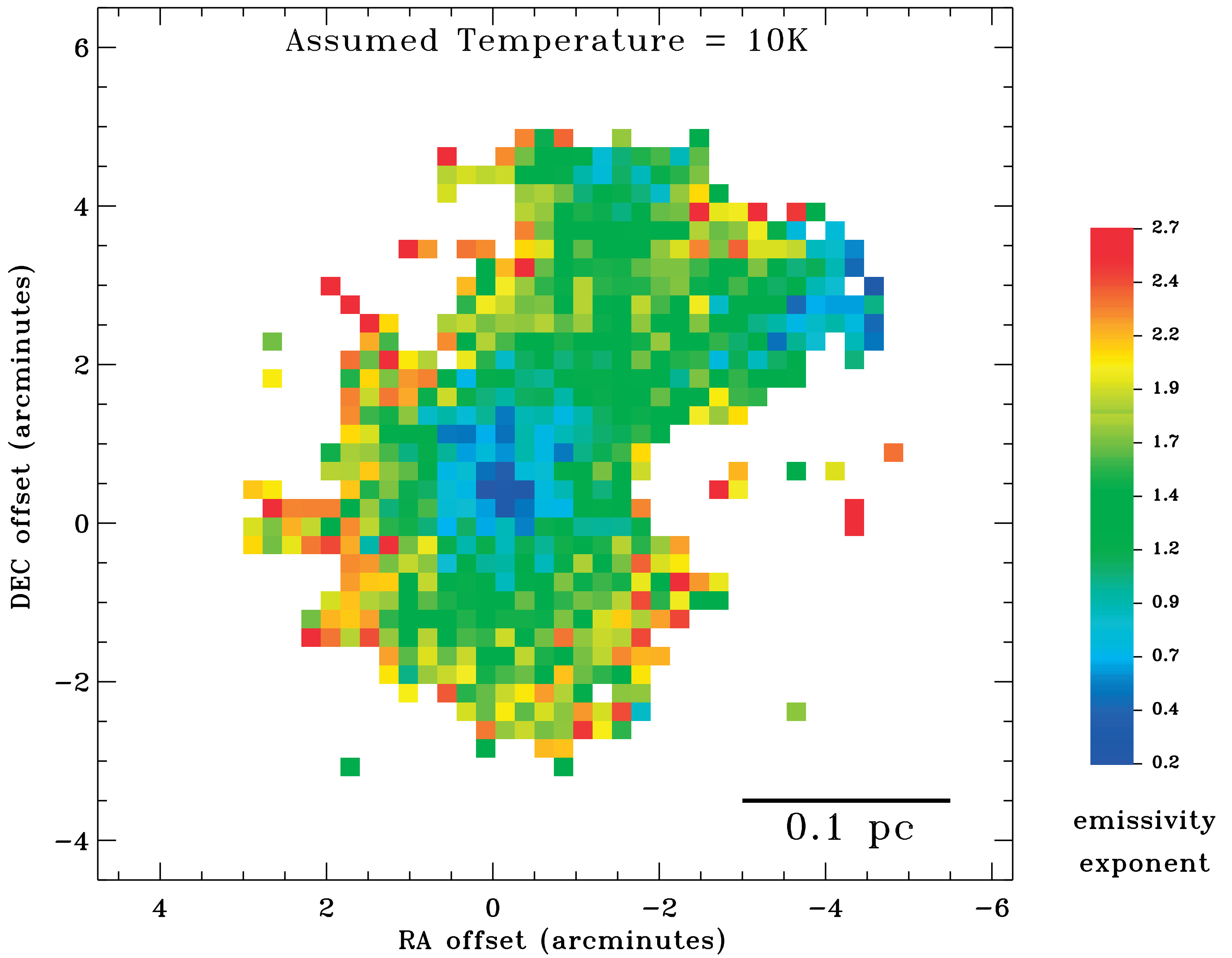


FIG. 5.—Emissivity spectral index ($\beta$) of the dust as determined by the 450 and 850 $\mu$m SCUBA maps with the assumption that the dust temperature is constant at 10 K.

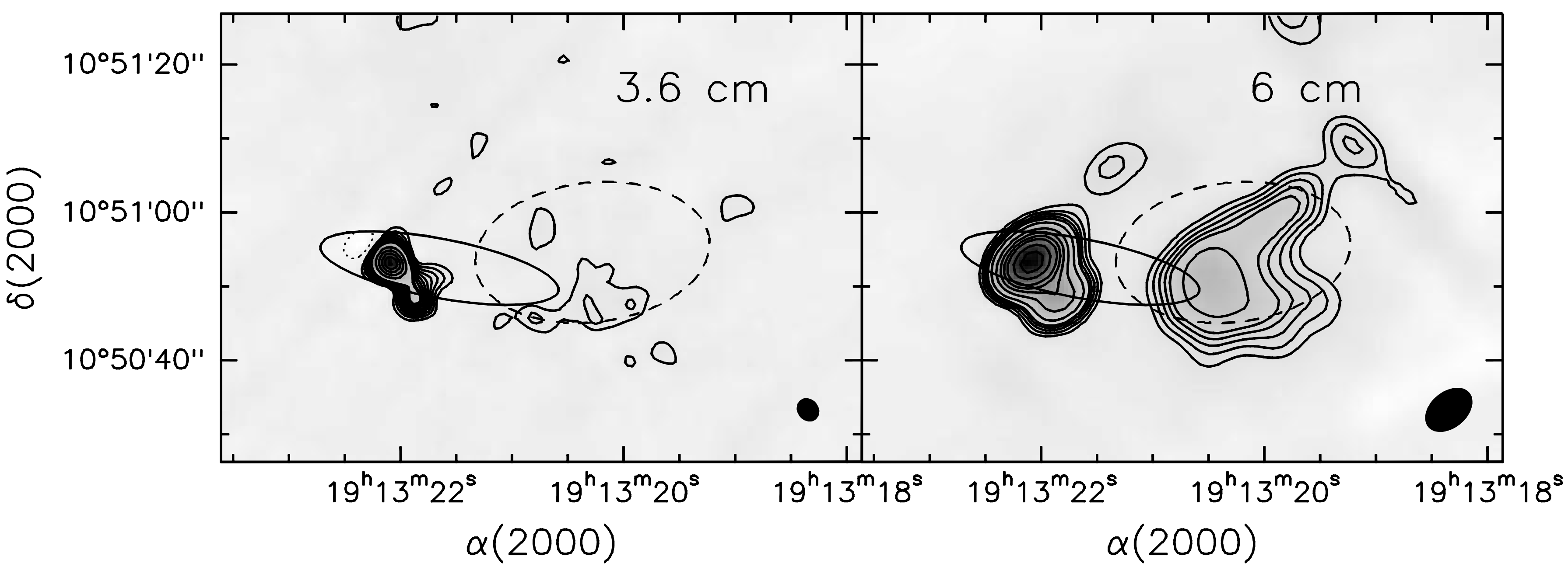


**Fig. A3.** 3.6 and 6 cm maps of the extended source G045.066+0.138 (30), and the compact sources G045.070+0.132 (11) and G045.072+0.132 (12); contour levels are −8, from 8 to 50 by 5 and from 50 to 300 by 50 mJy/beam at 3.6 cm, and −10, from 10 to 22 by 3, from 30 to 90 by 15, 120 and 150 mJy/beam at 6 cm. The filled ellipse represent the IRAS-PSC error box

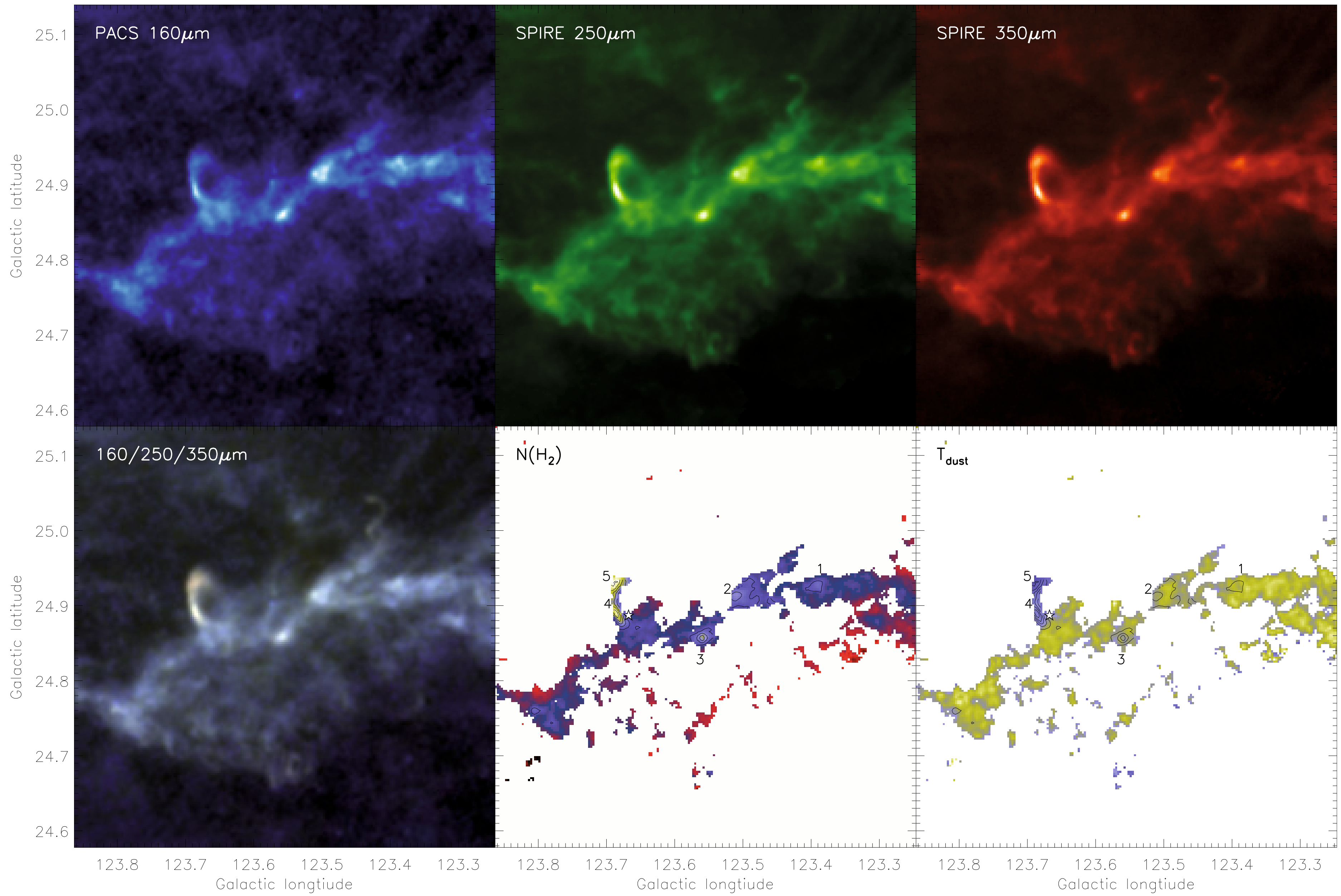


**Fig. 1.** The densest part of the Polaris Flare region at some of the observed wavebands. *Upper row*: 160 $\mu$m from PACS, and 250 $\mu$m and 350 $\mu$m from SPIRE. *Lower row*: false-colour image (where 160 $\mu$m is shown in blue, 250 $\mu$m is shown in green, and 350 $\mu$m is shown in red), column density map (where red is <4, blue is 4–8, and yellow is $>8 \times 10^{21}$ cm$^{-2}$), and colour temperature map (where blue is 10–11 K and yellow is 12–13 K). The contour levels on the column density map start at $4 \times 10^{21}$ cm$^{-2}$, and the interval between successive contours is $1.5 \times 10^{21}$ cm$^{-2}$. The same contours are repeated on the temperature map for ease of location. Five sources are seen above a column density of $4 \times 10^{21}$ cm$^{-2}$. These are labelled cores 1–5 (in order of increasing RA) on the last two panels and are discussed in the text. The loop (loop 1) discussed in the text (containing cores 4 & 5) is clearly visible in all images. The reddest features on the false-colour image are the coldest, and the loop shows up clearly as redder than the surroundings. Likewise in the temperature map, the loop shows up as blue, indicating that it is the coldest feature on the map. The position of the IRAS source (IRAS 01432+8725) is marked with a star on the last two panels (adjacent to core 4).

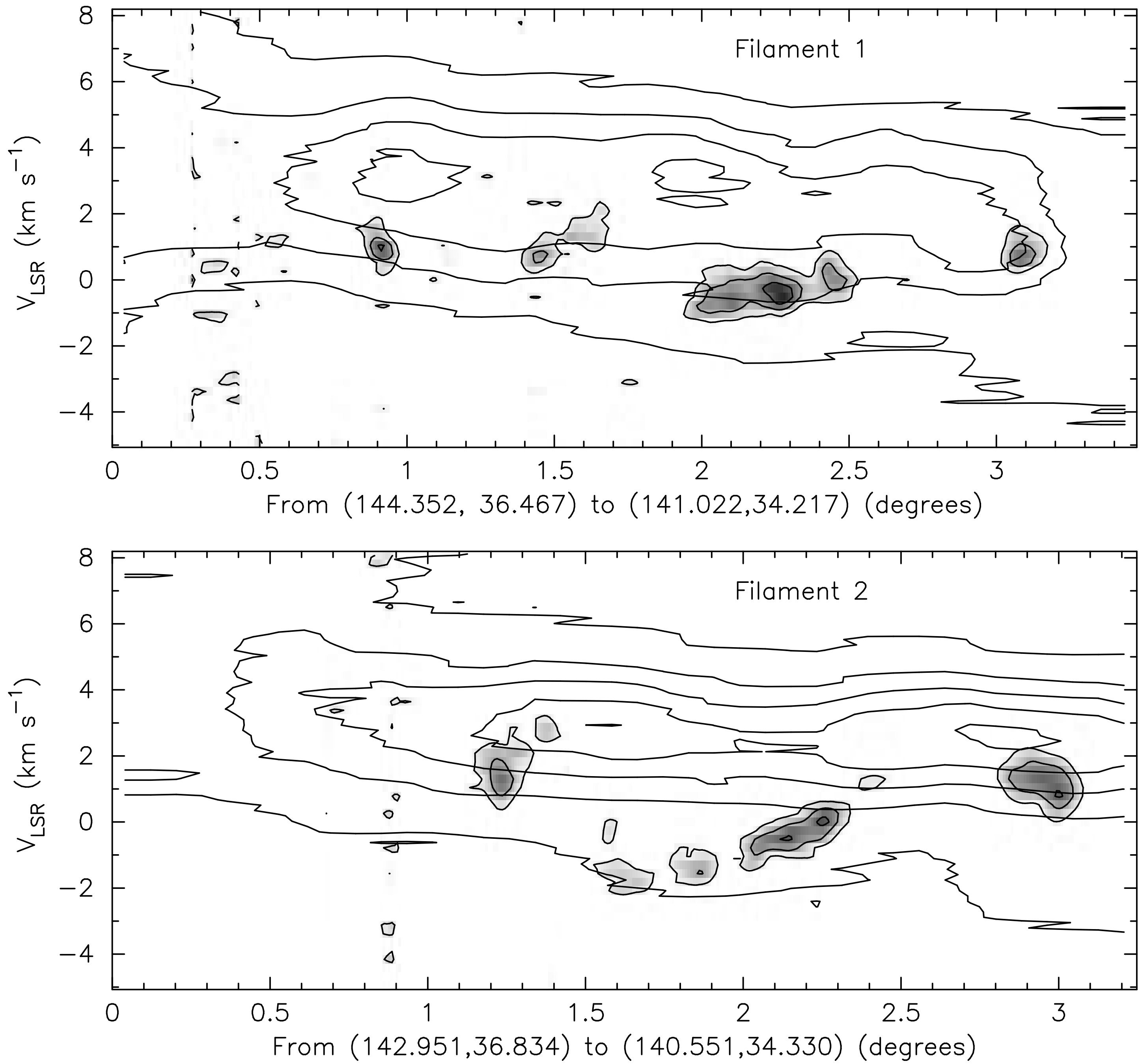


FIG. 15.—Position-velocity cuts of H I (*contours*) and CO (*gray scale*) in Filament 1 (*upper panel*) and Filament 2 (*lower panel*). See Fig. 6 for the orientation of the cuts. The CO and H I centroid velocities differ by up to 4 km s$^{-1}$, with the CO blueshifted with respect to the H I. This is evidence that the clouds have interacted with the wind, causing the expansion of the NCP loop. H I contours are at 4, 8, . . . , 20 K and CO contours are at 1, 2, 3 K. The CO data have been smoothed with a conical filter with interpolation radius 3′.

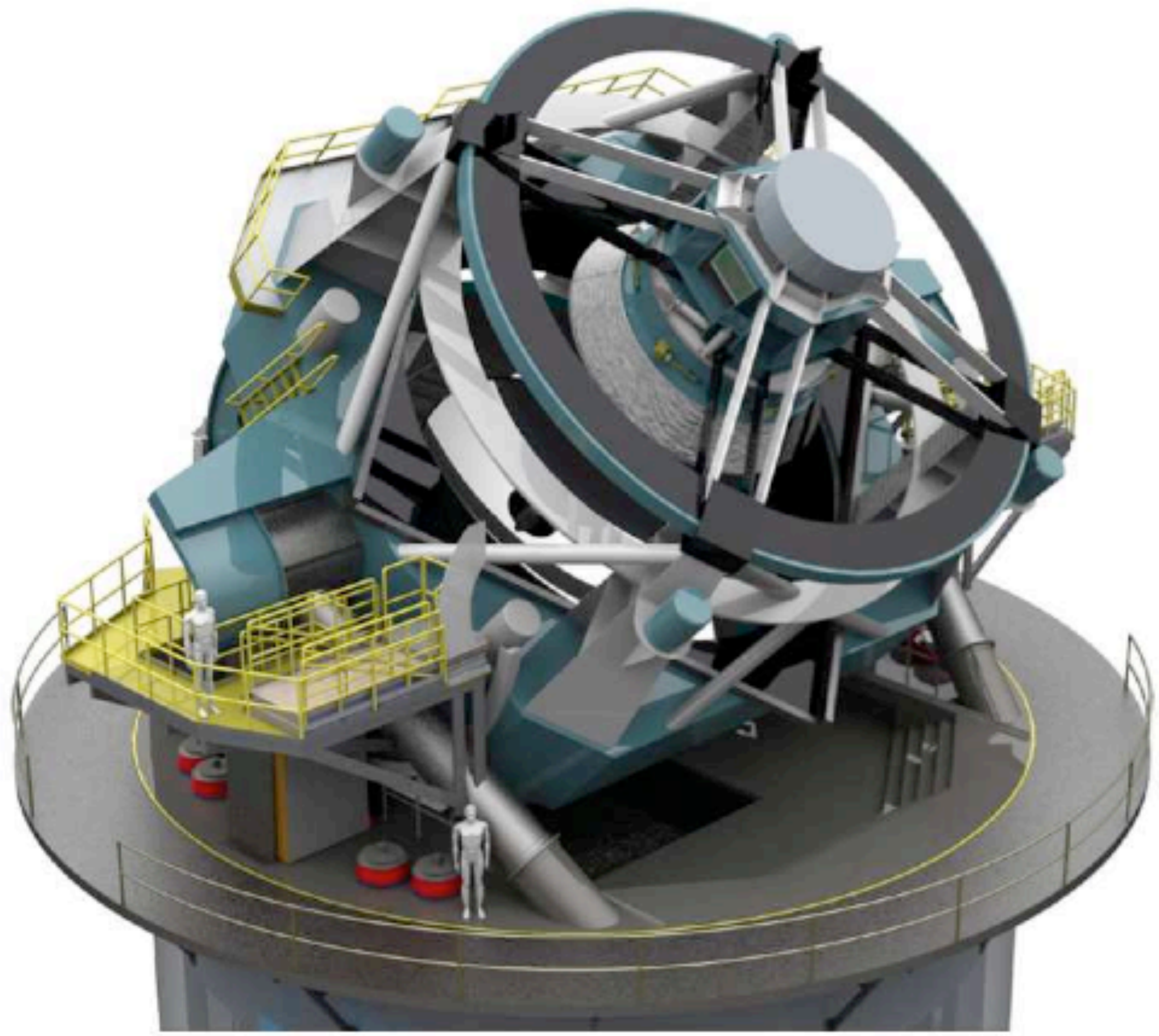

FIG. 8.— The baseline design (modified three-mirror Paul-Baker) for the LSST telescope.


DATA VIEWERS

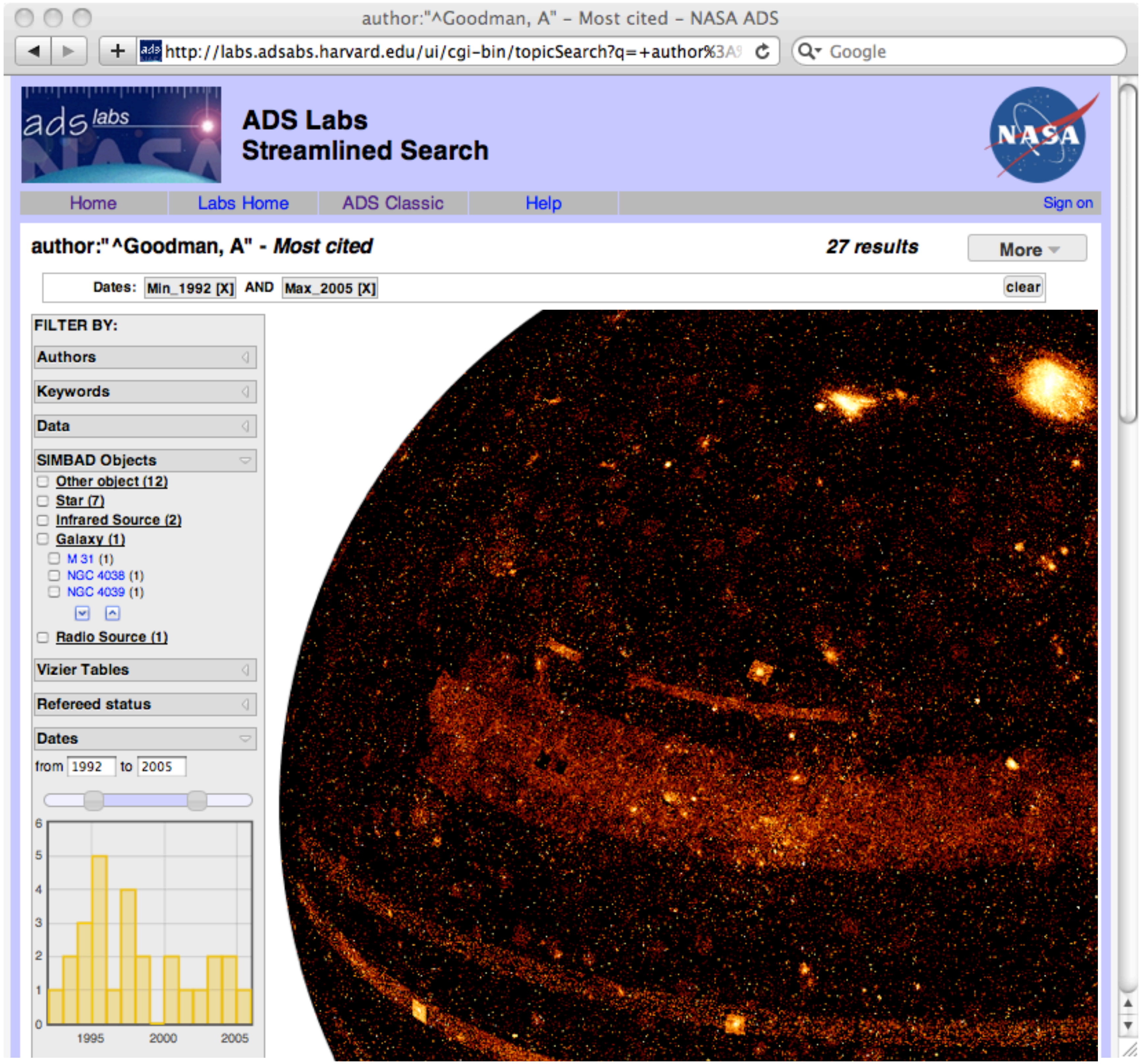


# FACETED ALL-SKY HEATMAP

*enables visual discovery*

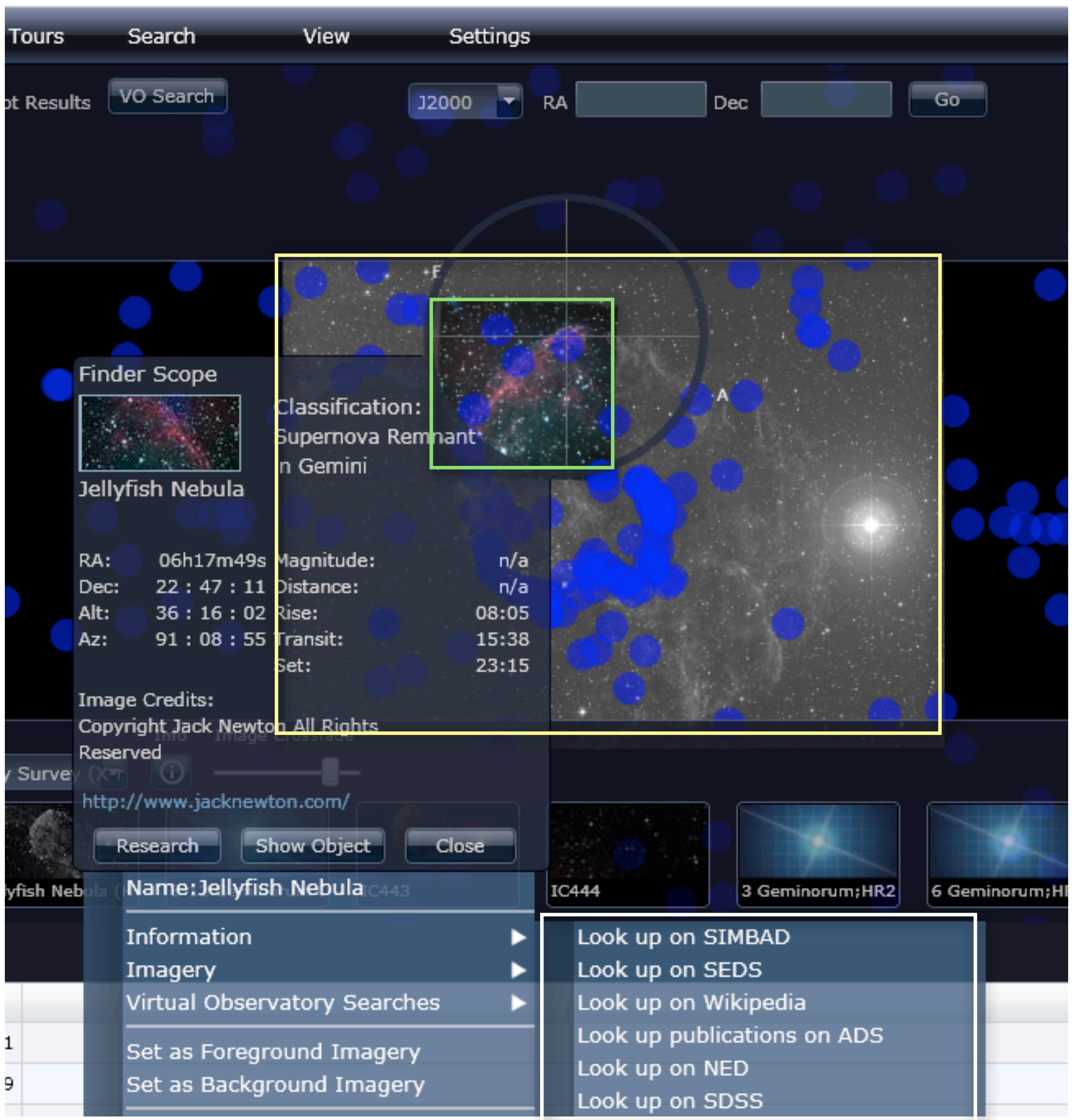


# HISTORICAL ALL-SKY IMAGE LAYER

*enables synoptic monitoring of astrophysical events*

# THANK YOU

*Alberto Pepe*
Postdoc, Harvard CfA
Co-founder, ***Au***thorea